Equatorial Currents in the Pacific 1950 to 1970 and Their Relations to the Trade Winds[1]

KLAUS WYRTKI

Dept. of Oceanography, University of Hawaii, Honolulu 96822

(Manuscript received 29 November 1973, in revised form 14 February 1974)

ABSTRACT

The mean meridional profile of dynamic topography across the zonal currents of the equatorial Pacific Ocean is disturbed by the observed deviation of monthly sea level at island stations from the long-term mean. From these monthly profiles the sea level difference across the major zonal currents for the period 1950–70 can be derived. A strong seasonal signal is apparent in the intensity of the currents, as well as large short- and long-term anomalies. Most of the energy of the currents is in the low frequencies. The North Equatorial Current and the Countercurrent fluctuate synchronously and in opposition to the South Equatorial Current. The fluctuations of the currents are related to the trade winds and are more strongly influenced by the position of the trade winds than by their strength. When the northeast trades are strong and in a southerly position during the first half of the year, both the North Equatorial Current and the Countercurrent are weak; when the trades are weaker and in a more northerly position during the second half of the year, both currents are strong.

1. Introduction

Any attempt to understand the low-frequency dynamics of ocean circulation will require continuous monitoring of the major ocean currents. These currents fluctuate largely in response to the wind systems, and in turn are responsible by advection for re-distribution of the heat input of the ocean. Consequently, they play a major role in the coupling of the entire ocean-atmosphere system in large time and space scales. Direct observations of the transports of ocean currents are difficult and expensive. Eulerian current measurements, because of high-frequency motion and low spacial coherence, cannot be used easily to compute and monitor transports in the open ocean over long periods of time. Geostrophic transport computations are more representative but routine gathering of such data is extremely elaborate and expensive, even if done by networks of moored buoys. Monitoring of transports of open ocean currents by electromagnetic methods has not yet been successfully accomplished. Surface trajectories of drifting buoys interrogated by satellites will certainly improve our knowledge about ocean circulation, but will probably not be suitable for the computation of transports.

In this study I will attempt to demonstrate that observations of sea level at oceanic islands can be used in conjunction with the mean dynamic topography to monitor the strength of major ocean currents in the equatorial Pacific Ocean. I will also show that both seasonal and long-term fluctuations of the equatorial currents are largely dependent on the location of the trade wind systems rather than on the strength of the winds.

2. Method and data

The relation between the transports of the Equatorial Countercurrent and the sea level difference between Christmas Island and Kwajalein was explored in an earlier article (Wyrtki, 1973) and a 21-year time series of Countercurrent transport was derived. The correspondence between seasonal variations of sea level and dynamic heights in the equatorial Pacific Ocean was demonstrated in another article (Wyrtki, 1974), and it was shown that the strength of the North Equatorial Current can be monitored by the sea level difference between Honolulu and Kwajalein, and that fluctuations of the North Equatorial Current and of the Countercurrent are synchronous. To monitor the fluctuations of the entire equatorial current system of the Central Pacific Ocean for each month of the period 1950–70, the following method is proposed: the profile of average annual dynamic height of the sea surface relative to 500 decibars (db) will be disturbed by the deviation of the sea level in each individual month from its long-term mean. These monthly sea level profiles will be used to determine the height of sea level at the various ridges and troughs associated with the equatorial circulation, which is essentially zonal. The differences of sea level height between subsequent topographic features will be considered indices for the strength of the different equatorial currents.

A map showing the dynamic topography relative to

[1] Hawaii Institute of Geophysics Contribution No. 601.

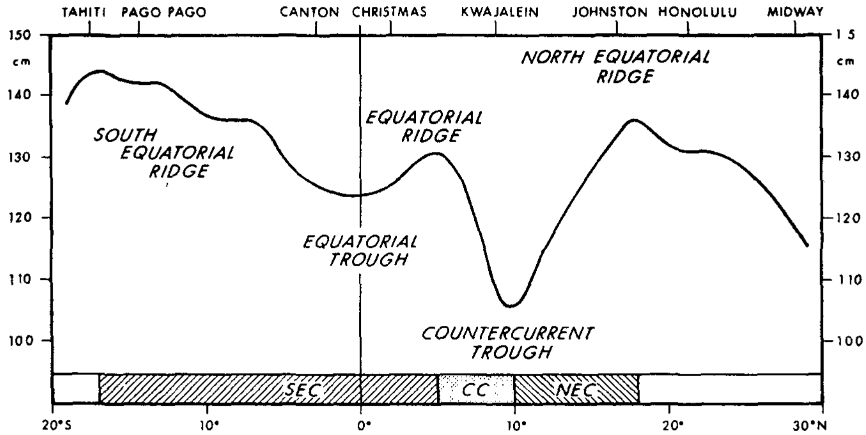

FIG. 1. Meridional profile of dynamic height relative to 500 db averaged zonally between 140W and 170E together with positions of sea level stations, topographic features, and currents.

500 db for the western equatorial Pacific Ocean between 30N, 20S, 140E and 140W based on approximately 6900 hydrographic stations (Wyrtki, 1974) shows that zonal circulation takes place between the following ridges and troughs: the North Equatorial Ridge near 19N, the Countercurrent Trough near 10N, the Equatorial Ridge near 3N, the Equatorial Trough at the equator, and the South Equatorial Ridge near 15S. Because of this pronounced zonal structure the dynamic heights on which the map is based have been zonally averaged between 170E and 140W over 50° of longitude; the resulting profile of dynamic height is shown in Fig. 1 together with the location of eight island stations for which long sea level records are available. From the records of monthly mean sea level at each station the long-term mean for the period 1950–70 was subtracted, forming the anomaly of sea level for that particular month and station. The sea level anomaly was then linearly interpolated in the north-south direction between the stations and superimposed on the mean annual dynamic topography. Table 1 summarizes some data relevant to the sea level stations. The standard deviation of the sea level anomalies is typically 5 cm, with Johnston Island being substantially higher because of its location near the center of the North Equatorial Current, the larger part of which can be either north or south of the island. Tahiti has the smallest standard deviation, probably because of its location in the rather stable South Equatorial Ridge. No corrections were applied for atmospheric pressure, which fluctuates only slightly in tropical regions and has been found by Roden (1963) to be rather poorly related to sea level in the equatorial zone, a result we can confirm and which is clearly indicated by the low standard deviation of atmospheric pressure at the stations shown in Table 1.

From the monthly profiles of sea level the position and sea level height at the five ridges and troughs characterizing the profile were determined and are shown in the form of time series in Fig. 2. The difference in sea level between successive ridges and troughs, which are

TABLE 1. Characteristic parameters for sea level stations used in this study. All values in centimeters.

Station	Latitude	Period	Coherence	Extreme sea level Maximum	Extreme sea level Minimum	Standard deviation Sea level	Standard deviation Atmospheric pressure	Remarks
Midway	28° 13′N	1950–70		+19	−22	6.3	3.1	
			0.22					
Honolulu	21° 18′N	1950–70		+16	−21	4.7	1.5	
			0.47					
Johnston	16° 45′N	1950–70		+17	−32	7.1	1.2	10 months missing
			0.04					
Kwajalein	8° 44′N	1950–70		+14	−24	5.4	1.0	
			−0.58					
Christmas	1° 57′N	1956–70		+17	−14	5.5	1.1	8 months missing
			0.85					
Canton	2° 48′S	1950–67		+16	−10	3.9	1.0	
			−0.12					
Pago Pago	14° 17′S	1950–70		+19	−17	5.4	1.7	
			0.12					
Tahiti	17° 32′S	1957–64		+11	−7	2.9	1.6	only 7 years of data

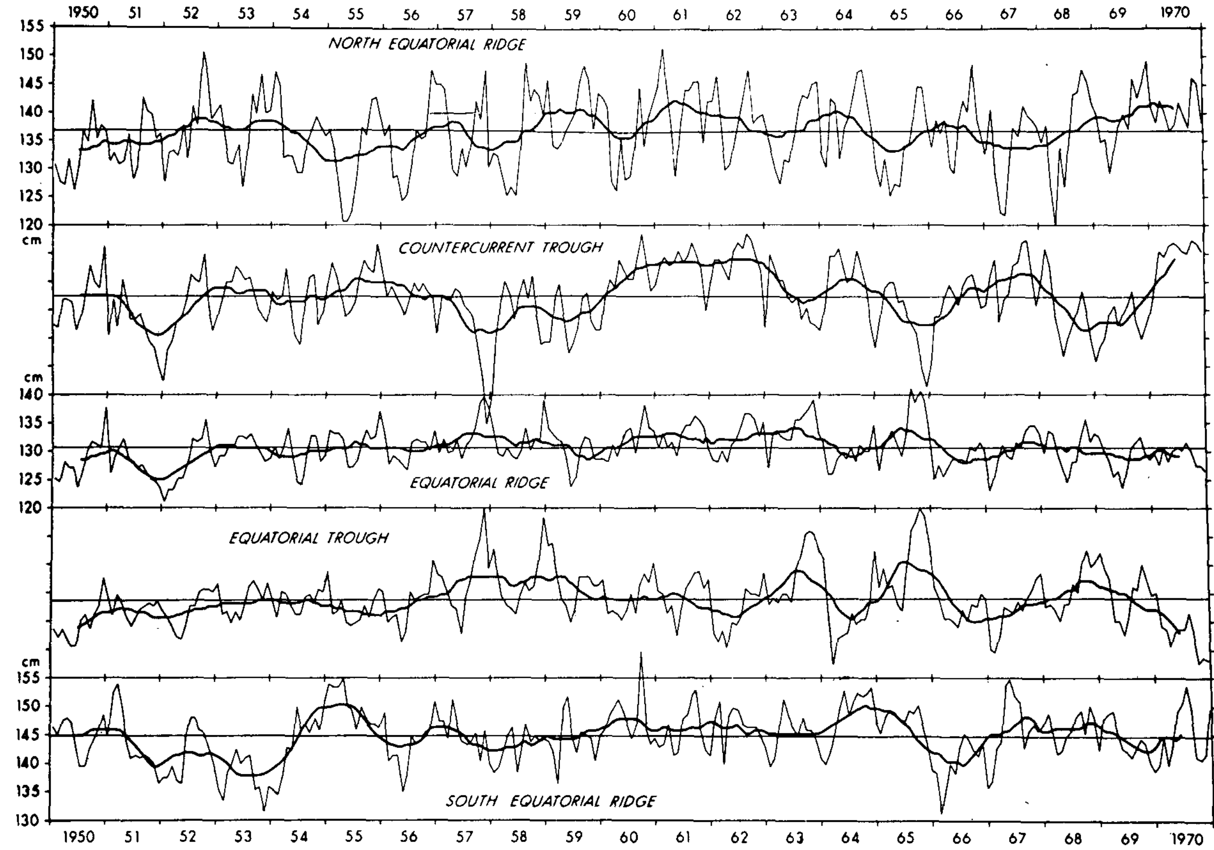

FIG. 2. Time series of sea level height (cm) at ridges and troughs associated with the equatorial circulation, 1950–70. Thin curves give monthly averages, heavy curves 12-month running means.

considered to represent indices for the strength of the respective currents, are shown as time series in Fig. 3.

3. Fluctuations at the topographic ridges and troughs

It is advantageous that most of the sea level stations are situated near the major topographic features of the mean sea level profile. The sea level height in the North Equatorial Ridge (Fig. 2) is essentially given by the sea level in Honolulu, although the position of the ridge fluctuates between 17 and 25N during the observation period. The seasonal cycle is very pronounced, but strong differences between individual years and long-term fluctuations are also apparent. In the Countercurrent Trough, which fluctuates in position only between 9 and 11N, the sea level height is practically determined by Kwajalein. Seasonal effects are much less pronounced, and long-term variations are dominant. Especially apparent are the strong negative deviations, which coincide with warming of the eastern tropical Pacific and with the occurrence of El Niño (Wyrtki, 1973). Sea level height at the Equatorial Ridge is chiefly represented by the observations at Christmas Island; the fluctuations are rather small and a seasonal cycle is apparent. Long-term trends are not very pronounced. In the Equatorial Trough, sea level height is given by the average between Christmas and Canton Island, and sea level observations at both stations correlate with $r=0.85$. The seasonal cycle is pronounced, but it is overshadowed by strong short- and long-term departures. The positive departures which are most pronounced coincide with negative departures of the sea level in the Countercurrent Trough. The position of the trough may vary between 3N and 3S. Sea level heights in the South Equatorial Ridge are expected to be disturbed by the presence of the South Equatorial Countercurrent (Reid, 1961). The seasonal signal is very weak; long-term trends and short departures dominate. Some of the characteristics of sea level fluctuations at these topographic ridges and troughs are summarized in Table 2.

Correlations between sea level at the five ridges and troughs have been computed for monthly values as well as for 12-month running means and are given in Table 3. They are all very weak, showing no correlations among most of these features, except for a correlation of 0.72 between the Equatorial Ridge and Trough, and a correlation of −0.51 between the Countercurrent Trough and the Equatorial Trough. The latter demonstrates that the Equatorial Trough is filled when the

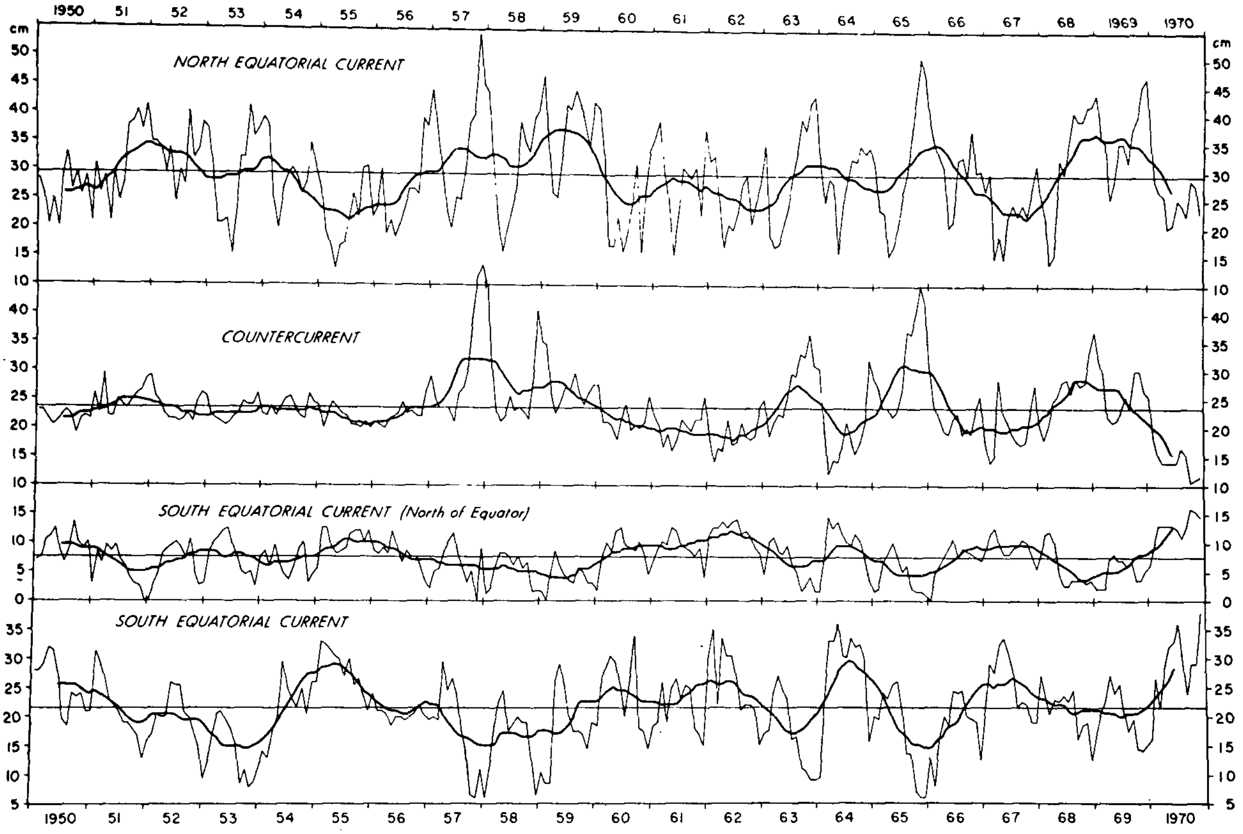

FIG. 3. As in Fig. 2 except for sea level difference across zonal currents of the western central equatorial Pacific, 1950–70.

Countercurrent Trough is deepened, thus indicating an inverse relation between the Northern and Southern Hemispheric circulation systems, which will be discussed later. The high correlations between these three features exist also in the long-term means.

4. Time series of the equatorial currents

Sea level differences between the successive ridges and troughs can now be calculated and will be considered a measure or index of the strength of the respective zonal currents. Between the North Equatorial Ridge and the Countercurrent Trough flows the North Equatorial Current; between the Countercurrent Trough and the Equatorial Ridge flows the Countercurrent. The South Equatorial Current flows to both sides of the equator, with the Equatorial Trough usually at the equator. Although the geostrophic approximation is no longer adequate close to the equator, and strong currents can be balanced by weak pressure gradients, the formal

TABLE 2. Characteristic sea level fluctuations at topographic ridges and troughs, and of sea level differences across currents in the western central equatorial Pacific. All values in centimeters.

	Mean	Departure Maximum	Departure Minimum	Variation in position		Standard deviation	Mean monthly maximum minus minimum
North Equatorial Ridge	137	+14	−17	25N	17N	6.6	12.3
Countercurrent Trough	107	+11	−22	11N	9N	5.8	7.4
Equatorial Ridge	131	+10	−10	5N	3N	3.5	4.7
Equatorial Trough	123	+17	−11	3N	3S	5.0	7.8
South Equatorial Ridge	145	+15	−14	13S	17S	4.8	3.4
North Equatorial Current	29	54	13			8.1	14.5
Countercurrent	23	53	10			5.9	7.6
South Equatorial Current (north of equator)	7	16	0			3.5	5.3
South Equatorial Current	22	38	6			6.7	10.0

TABLE 3. Correlation coefficients between time series representing equatorial currents, ridges and troughs. *Values in the upper right half give coefficients for the individual monthly values,* those in the lower left half for the 12-months running means. The ridge and trough associated with a particular current are outlined by a heavy border.

	North Equatorial Current	Equatorial Counter-current	S. E. C. North of Equator	South Equatorial Current	North Equatorial Ridge	Counter-current Trough	Equatorial Ridge	Equatorial Trough	South Equatorial Ridge	
North Equatorial Current		0.61	-0.69	-0.56	0.69	-0.63	0.06	0.52	-0.24	North Equatorial Current
Equatorial Counter-current	0.66		-0.87	-0.75	-0.01	-0.84	0.40	0.87	-0.10	Equatorial Counter-current
S. E. C. North of Equator	-0.81	-0.88		0.72	-0.05	0.88	-0.10	-0.77	0.18	S. E. C. North of Equator
South Equatorial Current	-0.63	-0.70	0.68		-0.18	0.57	-0.40	-0.76	0.62	South Equatorial Current
North Equatorial Ridge	0.50	-0.16	-0.01	-0.15		0.14	0.22	0.18	-0.07	North Equatorial Ridge
Counter-current Trough	-0.76	-0.86	0.91	0.60	0.19		0.16	-0.51	0.26	Counter-current Trough
Equatorial Ridge	-0.25	0.19	0.13	-0.14	0.05	0.33		0.72	0.25	Equatorial Ridge
Equatorial Trough	0.47	0.84	-0.70	-0.64	0.04	-0.49	0.62		0.03	Equatorial Trough
South Equatorial Ridge	-0.42	-0.19	0.28	0.75	-0.17	0.36	0.35	0.02		South Equatorial Ridge

procedure to form sea level differences between topographic features will be continued across the equator. There are two branches of the South Equatorial Current: the smaller one, north of the equator, is determined by the sea level difference between the Equatorial Ridge and the Equatorial Trough; the larger branch, south of the equator, is determined by the sea level difference between the Equatorial Trough and the South Equatorial Ridge. Data are not sufficient to resolve the narrow and irregular South Equatorial Countercurrent.

There are pronounced differences and some important similarities among these four currents, and some statistical data are given in Tables 2 and 3. The North Equatorial Current is the strongest, exhibits the largest fluctuations, and has the strongest seasonal signal. The Countercurrent normally shows much smaller fluctuations and only a weak seasonal signal, but its anomalous excursions are all toward a stronger flow, are large, and are confined to only a few cases. The strength of the two currents correlates at 0.61 for monthly means and at 0.66 for the 12-month running mean, which indicates that the two currents fluctuate essentially synchronously; the long-term trend of the two currents is practically the same (Fig. 3). The power spectra of the two currents and their coherence spectrum up to 6 cycles per year (cpy) are shown in Fig. 4a, and demonstrate that most of the power is in the low-frequency fluctuations. There are marked peaks at the yearly and semiannual periods and coherence is highest for frequencies below 1 cpy. Coherence between the two currents is lowest between 2 and 4 cpy; the phase relation is zero throughout the spectrum. Sea level difference across the North Equatorial Current correlates well with sea level both at its northern and southern flank, but it is noteworthy that in the long term it correlates better with sea level in the Countercurrent Trough at −0.76 (Table 3).

The South Equatorial Current, which flows to both sides of the equator, is covered by our investigation only in its western region, where it is weaker than east of 140W, and where it is partially disturbed by the South Equatorial Countercurrent. The southeast trade winds as well as the South Equatorial Current are strongest to the east of 140W, and we do not wish to imply that the statements made in the following apply equally to the strongest part of the South Equatorial Current. Unfortunately, there are no sea level stations available to the east of 150W to enable investigation of its strength there.

Because of the existence of the Equatorial Trough, the sea level difference across the South Equatorial Current has to be formed in two parts. The main part of the South Equatorial Current is given by the difference between the South Equatorial Ridge and the Equatorial Trough; the smaller part north of the equator is given by the difference between the Equatorial Trough and the Equatorial Ridge. The sea level difference across the South Equatorial Current is smaller than that across the North Equatorial Current, at least at the longitudes considered, but this does not imply that the surface current speed or the volume transports are smaller, because the sea level difference is measured at a lower latitude having a smaller Coriolis parameter. The spectra of the two currents are almost identical, except that the peak at 2 cpy is missing in the South Equatorial Current (Fig. 4b). The coherence between the two currents is strong at low frequencies and weak at high frequen-

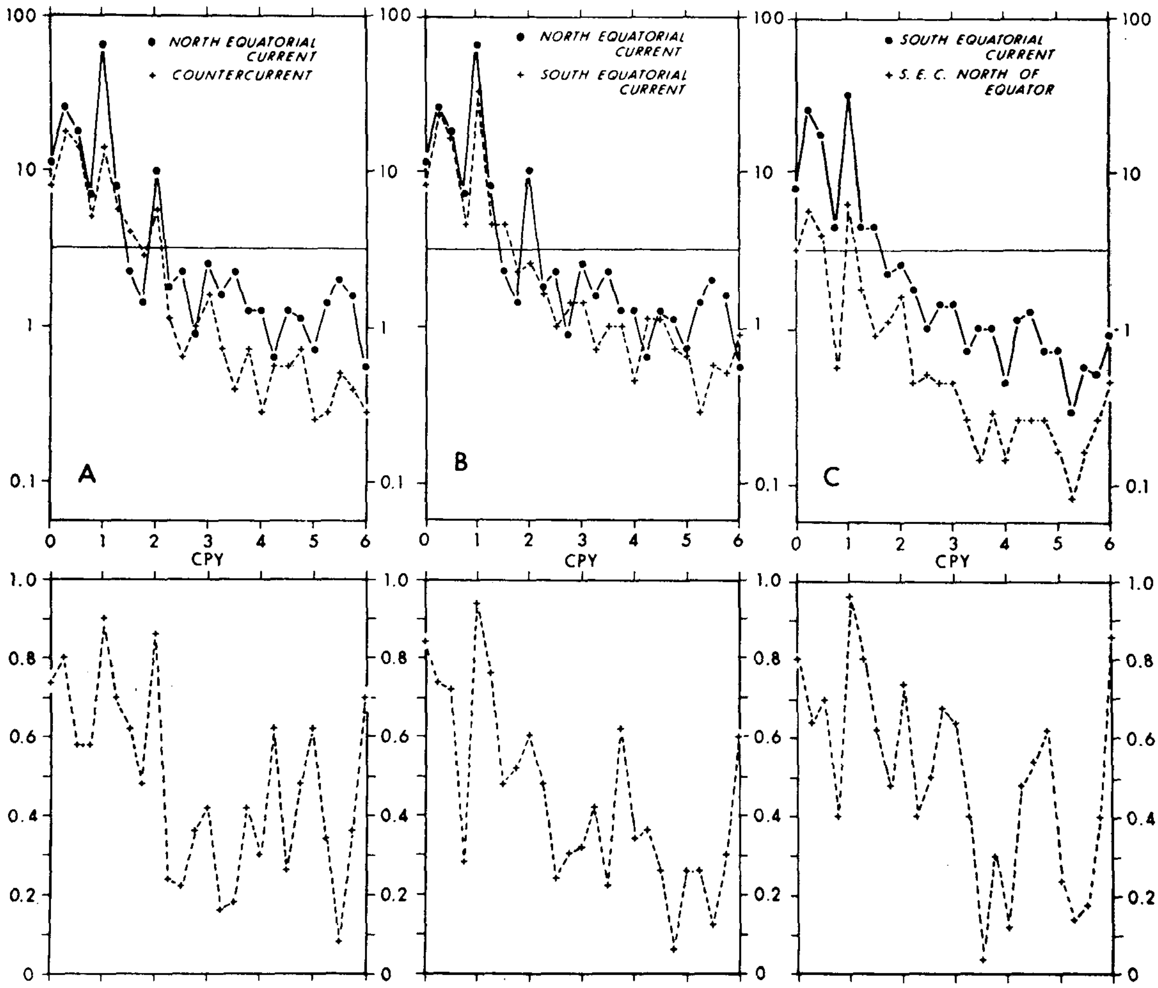

FIG. 4. Power spectra and coherence for zonal currents in the western central equatorial Pacific.

cies; the phase is 180° at low frequencies and irregular at high frequencies. The strength of the South Equatorial Current is determined about equally by the sea level at its northern and at its southern flank, both in the short as well as in the long term (Table 3).

The part of the South Equatorial Current situated north of the equator is relatively weak and shows some seasonal fluctuations, but is highly correlated with the South Equatorial Current south of the equator at zero phase shift (Fig. 4c). It should be noted that this part of the South Equatorial Current correlates well with sea level in the Equatorial Trough, but not with sea level at the Equatorial Ridge. Consequently, one must conclude that the Equatorial Trough determines and is a measure for the whole South Equatorial Current, both north and south of the equator.

The power spectra indicate quite clearly that most of the energy in the fluctuations of these currents is in the long periods or low frequencies (Fig. 4). The correlation coefficients in Table 3 also indicate that both portions of the South Equatorial Current fluctuate synchronously, as do the North Equatorial Current and the Countercurrent, and that the Northern Hemisphere current system fluctuates out of phase with the South Equatorial Current, a result previously derived by consideration of the seasonal signal only (Wyrtki, 1974). Surprisingly, the highest correlation is found between the neighboring Countercurrent and the northern part of the South Equatorial Current, due to the negative correlation between the Equatorial and the Countercurrent Troughs.

5. Relations to the wind field

Since horizontal circulation in the surface layer of the ocean is chiefly governed by the winds, it appears necessary and promising to investigate relations between the equatorial currents and the trade winds. At present, only mean wind or wind stress data are available and these will be used in this study. In progress is an investigation of the wind field in individual months, which will be used to study the development of selected events.

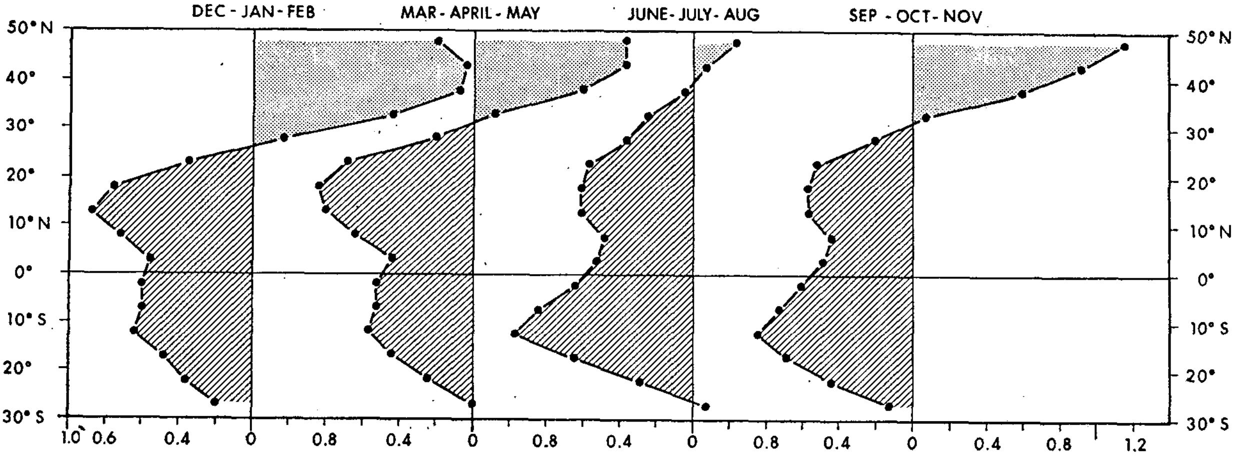

FIG. 5. Zonal component of wind stress in the Pacific Ocean according to Hellerman (1967), averaged between 160E and 140W at 30N to between 150 and 90W at 30S.

Seasonal variations of the trade winds have been investigated by Crowe (1951a, b), and quarterly mean values of wind stress over the oceans have been given

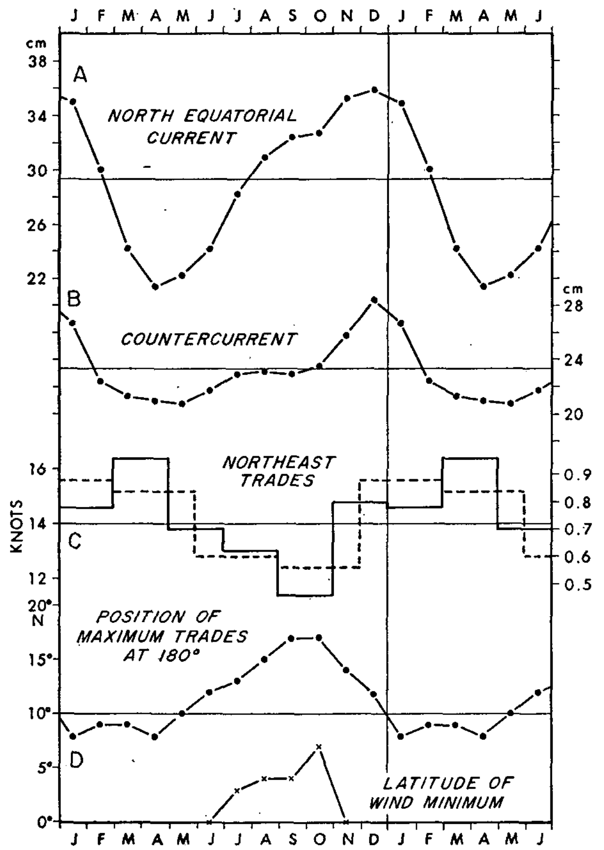

FIG. 6. Mean annual variation of sea level difference across the North Equatorial Current (A) and Countercurrent (B); of wind speed of the northeast trades according to Crowe (1951b) (C, solid line), and of maximum wind stress according to Hellerman (1967) (C, broken line); and of position of the maximum of the northeast trades and the minimum of zonal winds (D).

by Hellerman (1967). According to the maps given by Crowe (1951a), the maximum strength of the northeast trades over the Pacific Ocean occurs between 120W and 150E, while the maximum strength of the southeast trades occurs much further east, between 80 and 150W. In order to achieve a comparable meridional profile of the wind, we have zonally averaged the east-west component of wind stress given by Hellerman (1967) in a trapezoidal region between 160E and 140W at 30N to between 150 to 90W at 30S. The meridional profiles of zonal wind stress for each quarter are shown in Fig. 5. These profiles show clearly that the northeast trades are strongest in the first half of the year, and the southeast trades are strongest in the second half. They also show that the wind minimum between the two trade wind systems is a rather weakly developed feature. More important for our study, however, is the fact that the northeast trades fluctuate seasonally by more than 5° of latitude. This fact is more clearly shown in the monthly maps of trade winds presented by Crowe (1951a); from his maps the position of the trade wind maximum at 180° has been extracted and is given in Fig. 6. This figure also shows the seasonal variation of the strength of the northeast trades (kt) according to Crowe (1951b) for bimonthly periods, and the zonally averaged wind stress maximum according to Hellerman (1967), as well as sea level differences characterizing the strength of the North Equatorial Current and of the Countercurrent. It is apparent that during the first half of the year both currents are weak when the northeast trade winds are strong. At this time the trade wind belt is in a southerly position near 9N, and the minimum of zonal wind stress is near the equator. Consequently, the Countercurrent is being weakened by the opposing wind stress, and only part of the trade wind system acts on the North Equatorial Current. During the second half of the year, the trade wind belt is in a more northerly position (15N), and its full strength acts on the North Equatorial Current. Simultaneously, the Counter-

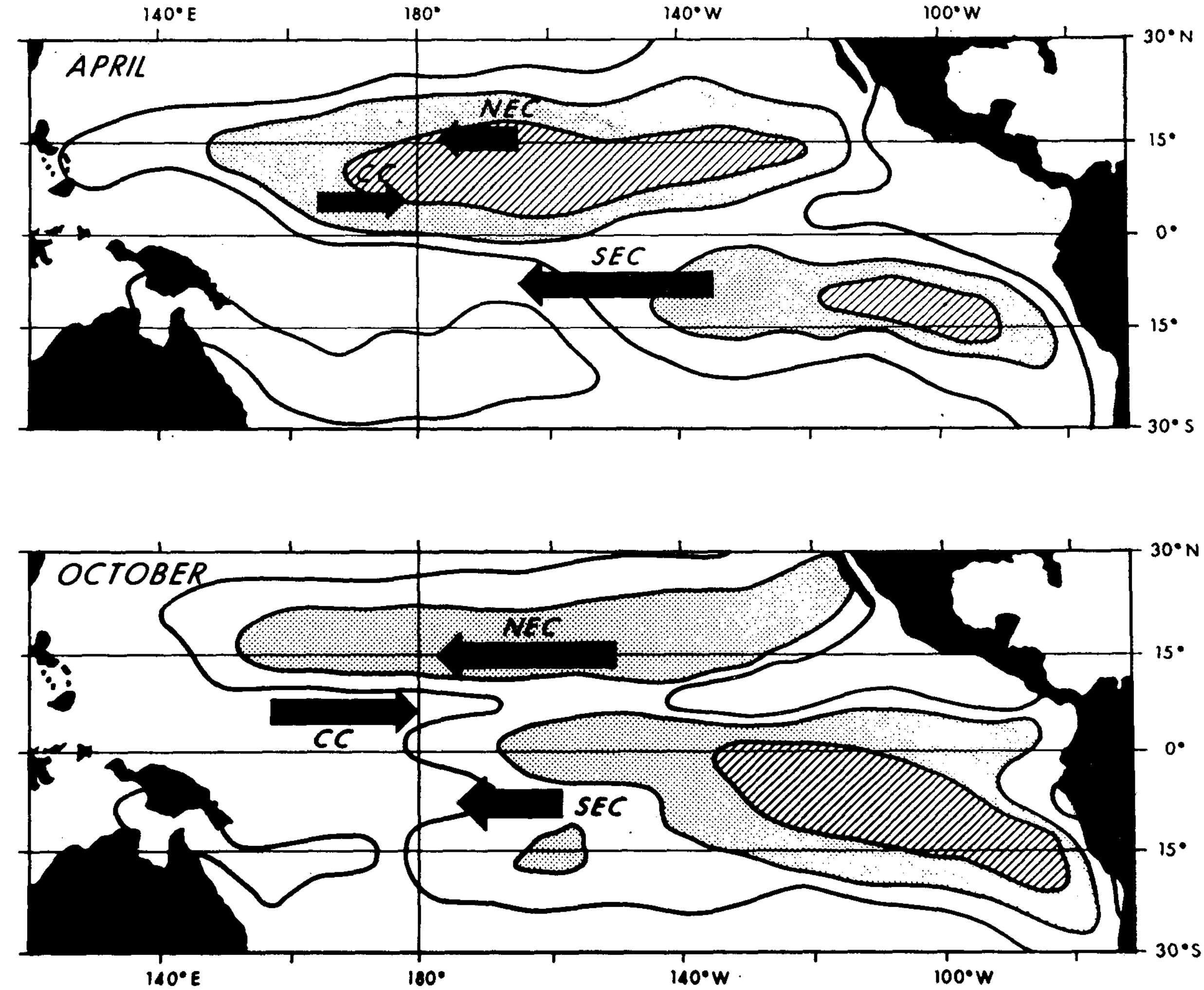

FIG. 7. Strength of equatorial currents in relation to the trade wind systems in April and October. Maps of the constancy of trade winds are according to Crowe (1951a), giving areas of 50%, 70% and 90% constancy of direction. Strength of currents is shown by relative length of arrows. NEC = North Equatorial Current, CC = Countercurrent, SEC = South Equatorial Current.

current can become stronger because it is no longer opposed by the strong trades.

These results have been summarized in Fig. 7, where the extent of the trade wind systems according to Crowe (1951a) is shown for April and October, as well as the relative strength of the three equatorial currents. From this figure it is apparent that the northeast trades are strongest in April, that they reach from the equator to 20N, and that their wind maximum is located near 10N. They oppose the Countercurrent, and contribute little to intensify the North Equatorial Current. There is no wind minimum between the two trade wind systems, except east of 140W. In October the northeast trades are clearly north of 10N, but are weaker than in April. They coincide completely with the North Equatorial Current and intensify it. At this time the Countercurrent is no longer opposed by the wind and, in fact, runs near the belt of minimum wind stress which clearly exists during this season.

A discussion of the dependence of the South Equatorial Current on the southeast trades is difficult, because this analysis relates only to its western portions between 140W and 170E, and not to the region where it is under the full influence of the southeast trades. In spite of this difficulty, some important conclusions can be inferred from Fig. 7. In October, when the southeast trades are strongest, they are also closest to the equator and even transgress it into the Northern Hemisphere. At this time, the South Equatorial Current is strongest near the equator (Wyrtki, 1965), at least to the east of 140W. Since the flow is strongest at the equator, this intensification is probably not indicated in the sea surface topography farther west. What is indicated by the sea surface topography is a relatively weak South Equatorial Current, which in October is not under the influence of strong trade winds (Fig. 7). In April, when the southeast trades are weaker and near 10S and do not transgress into the Northern Hemisphere, the South

Equatorial Current, at least as monitored by sea surface topography, is stronger in the western Pacific, because it lies in the direct continuation of the belt of strongest southeast trades. This relationship needs further study and documentation. In any case, the time series given in Fig. 3 for the South Equatorial Current should not be interpreted as an index for the entire current, but only for its western portion.

A more thorough analysis of the wind field in the equatorial Pacific is in progress, and in a successive paper I will explore the relations between winds and currents with particular attention to the Sverdrup theory, which should allow the computation of the zonal transports form the curl of the wind stress. Preliminary investigation does indicate, however, that this simple relation is not strictly satisfied. After analyzing the wind field for individual months, it is hoped that further empirical relations can be derived between the shifting wind field and the changing strength of the currents, especially during anomalous events.

Many of the sea level stations used in this study are not ideally situated with regard to the major current systems, and, in view of the great promise which sea level observations have for monitoring the changing circulation, additional stations will be established during the NORPAX project.

Acknowledgments. This research has been supported by the National Science Foundation and the Office of Naval Research under the North Pacific Experiment of the International Decade of Ocean Exploration; this support is gratefully acknowledged.

REFERENCES

Crowe, P. R., 1951a: The trade wind circulation of the world. *Trans. Inst. Brit. Geogrs.*, **15**, 39–56.

——, 1951b: The seasonal variation in the strength of the trades. *Trans. Inst. Brit. Geogrs.*, **16**, 25–47.

Hellerman, S., 1967: An updated estimate of the wind stress on the world ocean. *Mon. Wea. Rev.*, **95**, 607–614.

Reid, J. L., Jr., 1961: On the geostrophic flow at the surface of the Pacific Ocean with respect to the 1,000-decibar surface. *Tellus*, **13**, 489–502.

Roden, G. I., 1963: On sea level, temperature, and salinity variations in the central tropical Pacific and on Pacific Ocean islands. *J. Geophys. Res.*, **68**, 455–472.

Wyrtki, K., 1965: Surface currents of the eastern tropical Pacific Ocean. *Bull. Inter-Amer. Trop. Tuna Comm.*, **9**, 271–304.

——, 1973: Teleconnections in the equatorial Pacific Ocean. *Science*, **180**, 66–68.

——, 1974: Sea level and the seasonal fluctuations of the equatorial currents in the western Pacific Ocean. *J. Phys. Oceanogr.*, **4**, 91–101.